Photon-counting laser ranging with dual-comb asynchronous optical sampling

Yun Meng,[1,2] **Yanqing Shi,**[1,2] **Kai Zou,**[1,2] **Youjian Song,**[1,2,*] **Xiaolong Hu**[1,2,*]

[1]*School of Precision Instrument and Optoelectronic Engineering, Tianjin University, Tianjin 300072, China*
[2]*Key Laboratory of Optoelectronic Information Science and Technology, Ministry of Education, Tianjin 300072, China*
**Author e-mail address: yjsong@tju.edu.cn; xiaolonghu@tju.edu.cn*

Abstract: We report on laser ranging using dual-comb asynchronous optical sampling and a fractal SNSPD, achieving ranging precision of 7.7 micrometer and 65 nm with acquisition time of 1 ms and 1 s, respectively.

1. Introduction

Precise distance metrology plays an important role in many fields of scientific research and industrial manufacture. Laser ranging based on optical interferometry provides sub-wavelength precision but suffers from small non-ambiguity range. The alternative direct time-of-flight (ToF) measurement with laser pulses offers extended non-ambiguity range but typically with millimeter-level precision [1], limited by the bandwidth of photodetectors and timing electronics. The laser ranging scheme based on dual optical-frequency combs was proposed to combine the advantages of precise distance metrology of optical interferometry and large non-ambiguity range of ToF measurement [2]. In particular, the combination of dual-comb setup and time-correlated single-photon counting (TCSPC) technique improves the timing precision of single photons [3]. However, the relative long acquisition time poses a challenge to the mutual coherence and long-term stability of the combs since the distance is extracted from the photon-counting statistics obtained by TCSPC. In addition, the dual-comb interferometric setup suffers from the complex distance calculation because the ToF is obtained from the interferometric fringes through Fourier transform or Hibert transform [4].

In this paper, we demonstrate precise laser ranging combining dual-comb nonlinear asynchronous optical sampling (ASOPS) [4, 5] and photon counting using a fractal superconducting nanowire single-photon detector (SNSPD) [6]. Recently, the fractal SNSPDs have been demonstrated in ToF imaging [7], polarimetric measurements and imaging [8]. The implement of the fractal SNSPD in a dual-comb ASOPS setup overcomes the difficulty of maintaining long-term mutual coherence and complexity of distance determination in dual-comb interferometric setup based on TCSPC. We achieved indoor ranging precision of 7.7 µm with acquisition time of 1 ms, and 65 nm with acquisition time of 1 s.

2. Experiment and results

Figure 1 (a) presents the experimental setup for photon-counting dual-comb laser ranging by ASOPS. The central wavelengths of the signal laser and the local oscillator are 1568 nm, and 1570 nm, respectively. The repetition rate, f, of the signal laser is 134.271068 MHz, while the repetition rate of the local oscillator is slightly lower by Δf, making the local oscillator as ASOPS to the signal laser [5]. The ASOPS signals are extracted by two type-II PPKTP (periodically poled $KTiOPO_4$) crystals, one for the beam from the reference mirror (pulse train in Fig. 1 (b) with borders), and another for the beam from the target mirror (pulse train in Fig. 1 (b) without borders). As shown in Fig. 1 (b), the sum-frequency pulse is generated once the two pulses from the signal laser and the local oscillator overlap in the time domain. The ASOPS signal from the reference mirror is detected by a silicon photodetector (Si PD) with a bandwidth of 50 MHz. The pulses reflected by the target mirror have a time-of-flight delay, t_d, relative to the reference pulses. t_d is stretched to t_s in ASOPS signals with a magnification factor of $f/\Delta f$ in the time domain. The ASOPS pulses from the target mirror are coupled into an optical fiber and detected by the fractal SNSPD. The electrical signals from the Si PD and the fractal SNSPD, as illustrated in Fig. 1 (b), are fed into TCSPC to do start-stop measurement. Fig. 1 (c) presents the real-time waveform provided by the Si PD. Fig. 1 (d) presents the start-click rate measured by TCSPC at several Δf. At higher Δf, the start-click rate remains almost unchanged due to the lower amplitude of the start signal induced by inadequate sampling. The two combs can be phase-locked (PL) by a phase-locking loop, or work independently in a free-running (FR) mode. The measured drifts of Δf in PL mode and FR mode are shown in Fig. 1 (e).

Figure 2 presents the results of the photon-counting dual-comb laser ranging. The photon-counting statistics is recorded at a given acquisition time, as shown by an example histogram in Fig. 2 (a) with the acquisition time of 1 s and Δf of 30.006 kHz. The signal-to-noise ratio (SNR) is defined as the peak height of the coincidence

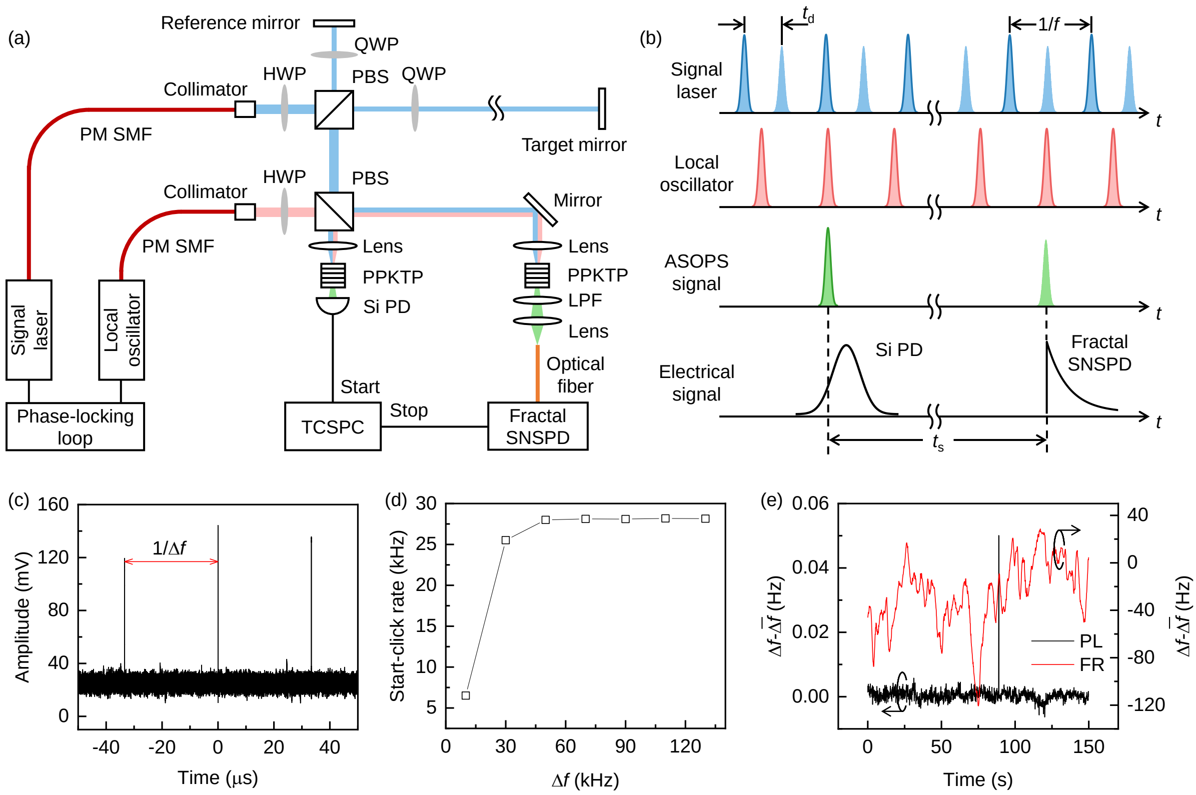

Fig. 1. Experimental setup, principle, and basic characterization of the photon-counting dual-comb laser ranging. (a) Schematics of the experimental setup. PM SMF: polarization-maintaining single-mode fiber; HWP: half-wave plate; PBS: polarization beamsplitter; QWP: quarter-wave plate; PPKTP: periodically poled $KTiOPO_4$; Si PD: silicon photodetector; LPF: low-pass filter; SNSPD: superconducting nanowire single-photon detector; TCSPC: time-correlated single-photon counting. (b) Principle of the time-of-flight measurement by asynchronous optical sampling (ASOPS). (c) Real-time waveform provided by Si PD. (d) Start-click rate measured by TCSPC at several repetition-rate differences, Δf. (e) Measured variation of Δf along time with the signal laser and the local oscillator in phase-locked (PL) mode and free-running (FR) mode.

between the two ASOPS signals divided by the peak of the noise floor. Fig. 2 (b) presents the zoom-in view of (a) with y-axis in the linear scale. We use the exponential-modified Gaussian (EMG) function to fit the coincidence peak, and the time corresponding to the maximum of the fitting curve is defined as t_s. Therefore, the measured distance can be calculated by $\frac{ct_s}{2n}\frac{\Delta f}{f}$, where c is the velocity of light in vacuum and n is the refractive index of the air, which is fixed to be 1. The EMG fitting to this specific histogram shows a full width at half maximum (FWHM) of 425 ps. At Δf of 30.006 kHz, the SNR of the histograms increases from 4.2 with acquisition time of 1 ms to 115.1 with acquisition time of 1 s, as shown in Fig. 2 (c).

For the stationary target mirror, we performed 20 measurements of target distance and calculated the Allan deviation. First, we investigated the Allan deviation of the measured distance at several Δf, at the acquisition time of 1 s. As shown in Fig. 2 (d), the Allan deviation reaches minimum at Δf of 30.006 kHz. Since the ranging accuracy scales up with $\Delta f/\sqrt{N}$ for given photodetectors, timing electronics and repetition rate of the signal laser, where N is the number of accumulated events in the coincidence peak, the ranging precision suffers from smaller N at lower Δf, and saturated N at higher Δf as shown in Fig. 1 (d). Therefore we fixed Δf to be 30.006 kHz in our following measurements. Fig. 2 (e) presents 20 measurements of the target distance at the acquisition time of 10 ms, 100 ms, and 1 s. The average measured distance is 47.404588 mm at acquisition time of 1 s. Fig. 2 (e) presents the Allan deviation of the measured distance at different acquisition time. The phase-locking loop enhances ranging precision, especially for long acquisition time, because the low-frequency noise such as drift of repetition-rate difference deteriorates the ranging precision. The Allan deviation is 7.7 μm with the acquisition time of 1 ms, and drops to be 65 nm with longer acquisition time of 1 s.

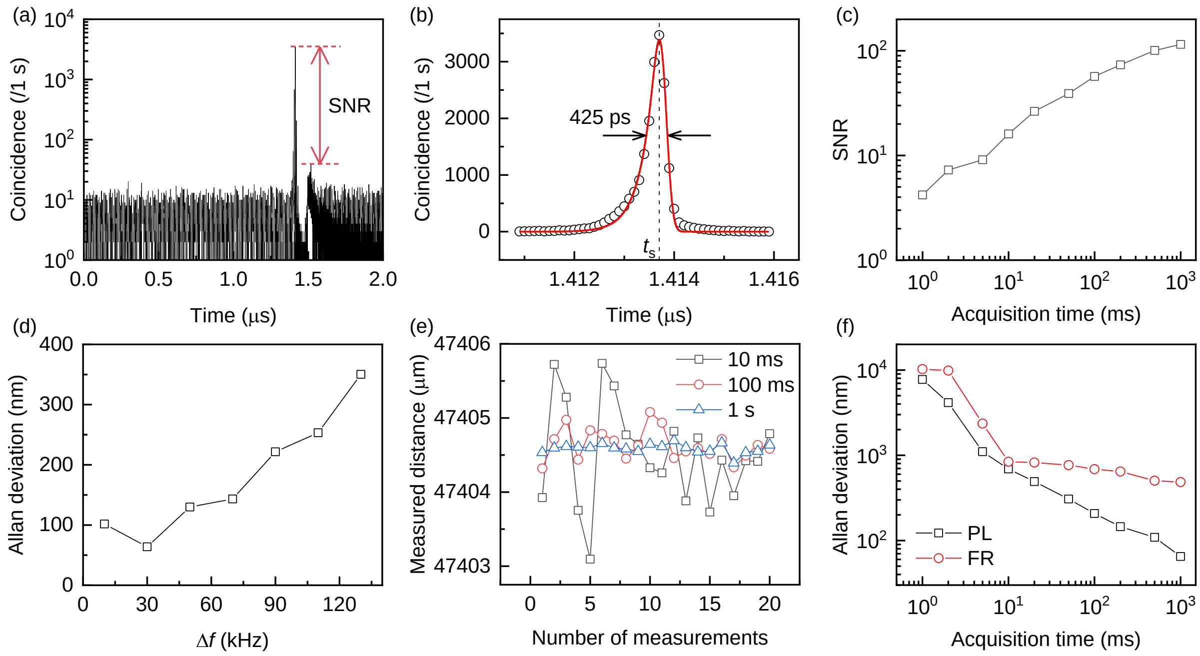

Fig. 2. Results of the photon-counting dual-comb laser ranging. (a) An example histogram of the start-stop coincidence, at the acquisition time of 1 s and Δf of 30.006 kHz. (b) Zoom-in view of the histogram in (a), with y-axis re-plotted in the linear scale. The exponential-modified Gaussian fitting to the coincidence peak shows a full-width at half maximum (FWHM) of 425 ps. (c) Signal-to-noise ratio (SNR) of the measured histograms versus acquisition time at Δf of 30.006 kHz. (d) Allan deviation of the measured distance versus Δf at the acquisition time of 1 s. (e) Twenty measurements of the distance at the acquisition time of 10 ms, 100 ms, and 1 s. (f) Allan deviation of the measured distance versus acquisition time at Δf of 30.006 kHz, with the signal laser and the local oscillator in phase-locked (PL) mode and free-running (FR) mode.

3. Conclusion

In conclusion, we demonstrat precise laser ranging with a dual-comb ASOPS setup and a fractal SNSPD. At the repetition rate of 134.271068 MHz and the repetition-rate difference of 30.006 kHz, the Allan deviation of the measured distance is 7.7 μm with acquisition time of 1 ms, and further reduces to 65 nm with acquisition time of 1 s. We plan to extend this method with high ranging precision to a longer distance in the future.

Acknowledgment

This work was supported by the National Natural Science Foundation of China (NSFC) (62071322).

References

1. S. Pellegrini, G. S. Buller, J. M. Smith, A. M. Wallace, and S. Cova. *Measurement Science and Technology*, 11(6):712, 2000.
2. I. Coddington, W. C. Swann, L. Nenadovic, and N. R. Newbury. *Nature Photonics*, 3(6):351–356, 2009.
3. X. Ren, B. Xu, Q. Fei, Y. Liang, J. Ge, X. Wang, K. Huang, M. Yan, and H. Zeng. *IEEE Photonics Technology Letters*, 33(1):27–30, 2020.
4. H. Zhang, H. Wei, X. Wu, H. Yang, and Y. Li. *Optics Express*, 22(6):6597–6604, 2014.
5. H. Shi, Y. Song, T. Li, C. Wang, X. Zhao, Z. Zheng, and M. Hu. *IEEE Journal of Selected Topics in Quantum Electronics*, 24(5):1102610, 2018.
6. Y. Meng, K. Zou, N. Hu, L. Xu, X. Lan, S. Steinhauer, S. Gyger, V. Zwiller, and X. Hu. *ACS Photonics*, 9(5):1547–1553, 2022.
7. K. Zou, Z. Hao, Y. Feng, Y. Meng, N. Hu, S. Steinhauer, S. Gyger, V. Zwiller, and X. Hu. *Optics Letters*, 48(2):415–418, 2023.
8. N. Hu, Y. Meng, K. Zou, Y. Feng, Z. Hao, S. Steinhauer, S. Gyger, V. Zwiller, and X. Hu. *Optica*, 9(4):346–351, 2022.